CHINESE OPTICS LETTERS

Vol. 23, No. 4 | April 2025

Method for measuring retinal capillary blood flow velocity by encoded OCTA

Shujiang Chen (陈淑江)[1,2], Kaixuan Hu (户凯旋)[1,2], Wei Yi (仪 维)[1,2], Fuwang Wu (吴付旺)[1,2], Yi Wan (万 熠)[1,2], Lei Zhang (张 磊)[1,2], Jianmei Li (李建美)[1,2], Aiqun Wang (王爱群)[1,2], and Weiye Song (宋维业)[1,2*]

[1] School of Mechanical Engineering, Shandong University, Jinan 250061, China

[2] Key Laboratory of High Efficiency and Clean Mechanical Manufacture of Ministry of Education, Shandong University, Jinan 250061, China

*Corresponding author: songweiye@sdu.edu.cn

Received July 30, 2024 | Accepted November 4, 2024 | Posted Online April 23, 2025

The quantification of microvascular blood flow velocity is pivotal in elucidating the characteristics of retinal microcirculation, and it plays a vital role in the early detection of numerous ophthalmic pathologies. However, non-invasive technology with a large field of view for directly measuring retinal capillary blood flow velocity is lacking. In this study, a novel imaging modality called encoding optical coherence tomography angiography (En-OCTA) is presented, utilizing retinal optical coherence tomography angiography (OCTA) encoding to accurately measure the absolute blood flow velocity in retinal capillaries. En-OCTA employs a scanning speed of 250 kHz to capture multiple OCTA images at two different locations on the same unbranched capillary. As red blood cells (RBCs) slowly flow through capillaries in a single file, intermittent light and dark changes can be observed on OCTA images. Analyzing the correlation of light and dark patterns in chronologically coded images of the capillary region allows for the determination of the lag time in RBC movement between two points. Combining this lag time with the distance between scan points allows the absolute blood flow velocity in the capillaries to be accurately calculated. Animal experiments demonstrate that the method can accurately measure capillary blood flow velocity and detect changes in velocity over the duration of anesthesia.

Keywords: capillary blood flow velocity; optical coherence tomography angiography; correlation of light and dark encode.
DOI: 10.3788/COL202523.041701

1. Introduction

The retinal capillary network is essential for maintaining vision and overall eye health, ensuring that the retina receives adequate nutrients and oxygen[1,2]. Abnormalities in retinal capillary blood flow velocity are associated with the onset and progression of various ophthalmic diseases[3] such as microvascular occlusive disorders[4] and diabetic retinopathy[5–7]. However, retinal capillaries are the smallest blood vessels in the posterior segment of the eye, with diameters of approximately 5–10 μm, which only allow red blood cells (RBCs) to flow slowly in a single-file manner[8,9]. This constraint poses significant challenges for the accurate measurement of blood flow velocity. Optical coherence tomography (OCT)[10–12], due to its non-invasive nature and high-resolution capabilities, has been widely employed to assess the structural and functional aspects of the retina. The advent of optical coherence tomography angiography (OCTA) has further extended OCT applications in imaging the retinal microvascular network, primarily providing structural information about retinal vessels[13,14]. Although OCTA significantly enhances the structural visualization of vascular networks and uses perfusion mapping as a method to estimate blood flow velocity, it still presents limitations in the precise quantification of blood flow velocity[15,16].

Several methods for quantifying retinal blood flow velocity have been proposed, including techniques based on the Doppler principle, fluorescence angiography, adaptive optics, and OCT signal analysis. Doppler-based OCT technology[17] has primarily been optimized for quantifying flow velocity in large vessels with continuous flow. Its application to retinal capillaries, which are small in volume and exhibit slow blood flow, is limited by the fact that most retinal capillaries are not axially oriented, a condition necessary for obtaining a Doppler signal[18,19]. To address these limitations, Tang *et al.*[20] developed an extended phase-resolved Doppler OCT to measure axial velocity in both large vessels and capillaries. This method requires extended acquisition time at each location to achieve a sufficient signal-to-noise ratio (SNR) for detecting the phase changes induced by the slowly flowing RBCs. To reduce acquisition time, Guo *et al.* proposed an OCT velocimetry method based on autocorrelation analysis for measuring axial blood flow velocity in capillary networks in the brain, requiring approximately 80 s of acquisition time and relying on

RBC-induced phase changes to derive the autocorrelation function[21]. Additionally, Srinivasan *et al.* introduced a method for estimating retinal capillary blood flow velocity using the OCT signal autocorrelation function, though it did not provide absolute velocity values[22]. Choi *et al.*[23] suggested an approach based on the decorrelation rate of OCT speckle signals to estimate RBC velocity in capillaries, using a capillary flow model to establish the relationship between decorrelation time and velocity. Hwang *et al.* utilized temporal autocorrelation fitting with OCTA to quantify retinal blood flow velocity, employing a simple temporal autocorrelation model to assess the decay constant as an indicator of blood flow velocity[24]. Adaptive optics imaging techniques can observe RBCs within retinal capillaries and detect blood flow velocity through their movement[25,26]. For instance, Zhang *et al.* non-invasively imaged RBC motion traces within vessels using an adaptive optics near-confocal scanning ophthalmoscope at a frame rate of 200 frame/s (fps) to measure blood flow velocity[27]. Neriyanuri *et al.* validated the application of commonly used adaptive optics methods in capillary flow analysis by comparing manual cell labeling with automated analysis of spatiotemporal information[28]. Despite its benefits, adaptive optics has a limited field of view and requires montage stitching, which can be time-consuming[24]. Song *et al.* observed intermittent fluorescent signals in retinal capillaries following the injection of a fluorescent agent[29] and used this method to quantify capillary blood flow velocity. Since this approach involves injecting fluorescent contrast agents, it carries inherent risks. In summary, most imaging techniques have limited fields of view when capturing capillary blood flow velocity and require multiple scans at a single location, leading to extended acquisition time. It is challenging to cover multiple capillary branches simultaneously, resulting in low acquisition efficiency. Additionally, fluorescence methods require the injection of contrast agents, which pose potential risks. Therefore, there is a need to develop a non-invasive, wide-field, and efficient method for measuring retinal capillary blood flow velocity.

In this work, we present a novel imaging modality called encoding optical coherence tomography angiography (En-OCTA), which utilizes retinal OCTA encoding to measure the absolute blood flow velocity in capillaries. This method can capture single or multiple capillaries at two locations within 6 s at a frame rate of 500 fps, allowing for non-invasive and accurate measurement of absolute blood flow velocity in retinal capillaries. Thus, the measurement field depends on the scanning range, and as long as capillaries at two distinct scanning locations are captured, the blood flow velocity can be calculated using the method described. The method and data processing procedure will be introduced, followed by the presentation of capillary blood flow velocity measurement results and demonstration of observed changes in retinal capillary blood flow velocity as anesthesia time increases.

2. Method

Figure 1 depicts our custom-built spectral-domain OCTA system, which features a superluminescent diode (SLD) light source

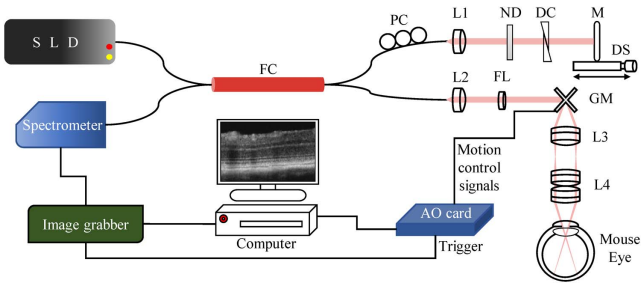

Fig. 1. The high-speed OCTA system. SLD, super luminescent diode; FC, fiber coupler; PC, polarization controller; L1, L2, collimating lenses; ND, neutral density filter; DC, dispersion controller; M, mirror; DS, displacement slide; FL, focus tunable lens; GM, two-dimensional scanning galvanometer; L3, achromatic doublet lens; L4, two achromatic doublet lens; AO card, analog digital card.

and a high-speed line-scan camera (Octoplus, e2v, Teledyne, UK), achieving an A-scan rate of 250 kHz. The camera data are transmitted to the image acquisition card (NI PCIe-1437). The motion control signals for the two-dimensional scanning galvanometer and the trigger signals for the image acquisition card were synchronously output by an analog digital (AO) card (NI, USB-6363). The spectral range of the system spans from 781 to 926 nm, the system's theoretical axial resolution is 2.21 μm, and the measured axial resolution is 2.3 μm.

Research indicates that RBCs exhibit single-file flow within capillaries[30], leading to intermittent light and dark variations in the capillary network on OCTA images (see the Visualization 1). The principle is shown in Fig. 2(a). Different scanning positions along the same unbranched capillary will exhibit similar light and dark changes over time. By determining the lag time of these changes between two locations and the distance between the scanning points, the absolute velocity of blood flow in the capillaries can be definitively calculated. To ensure the observation of intermittent capillary phenomena, the A-line speed is set at 250 kHz[31]. For high-speed OCTA, repeated scanning was performed at 512 B-scan positions. Each B-scan consisted of 200 A-lines, and each B-scan position was repeated four times. In the experiment, healthy wild-type mice (C57BL/6, 8 weeks old) were anesthetized with pentobarbital sodium. The experimental procedures were approved by the Ethics Committee of the School of Pharmacy, Shandong University (Approval No. 240008) on January 18, 2024. All animal care and experimental procedures adhered to ethical standards. During the experiment, hydration was used to keep the eyes moist, and a heating pad was employed to maintain body temperature. Figure 2(b) shows that, during scanning with a high-speed OCTA system, the collected OCTA images reveal intermittent capillaries and assist in localizing unbranched capillaries.

The standard angiography scanning protocol requires multiple rescans at the same location, but this rescanning process is time-consuming and may lead to potential issues such as the possibility of RBCs flowing past the second scanning position during repeated scans at the first location, which could subsequently impact the detection of changes in the brightness

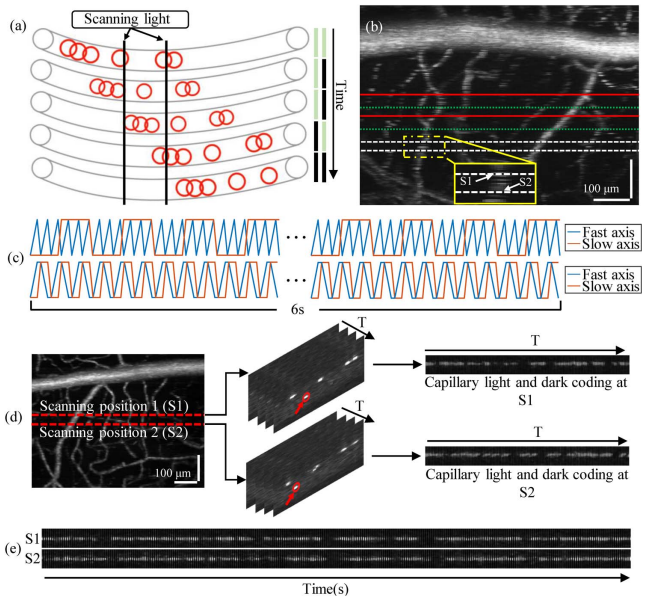

Fig. 2. (a) The light and dark changes of repeated scanning at two positions of a single capillary (repeat scanning 3 times for OCTA at each location). (b) High-speed OCTA image. The white dashed lines indicate the two scanning positions, and the yellow box illustrates the intermittent phenomenon produced by capillaries. The red solid lines and the green dashed lines represent two additional pairs of scanning positions that are equidistant from each other. (c) Different scanning protocols. The fast axis and slow axis waveforms are the signals that trigger the two galvanometers, respectively. (d) Capillary B-scan image processing at two locations. (e) Encoded images showing the variations in brightness over time of the same capillary cross-section at scanning positions S1 and S2.

coding of capillary images. To monitor blood flow velocity, the scanning protocol was modified to enhance the frame rate, leading to the introduction of a novel En-OCTA blood flow scanning protocol, as shown in Fig. 2(c). In this mode, alternating B-scans are conducted at two positions, with each B-scan on the fast axis being repeated only once. Alternating reverse scanning between locations S1 and S2 is performed, with the frame rate increased to approximately 500 fps, achieving at least a threefold enhancement, as shown in Table 1, where vps stands for volume/s and fps stands for frame/s.

The process is initiated by performing high-speed OCTA to capture angiographic images that are used to identify the same unbranched capillaries. Subsequently, repeated scans were performed using a modified En-OCTA scanning protocol at two locations on the same unbranched capillary, with 3000 B-scans per location. First, the scanning data from two different locations are separated, and the data from these scanning positions are reconstructed into individual angiographic images using optical microangiography (OMAG)[32]. To ensure consistent and complete capture of capillary cross-section images, regions containing capillary cross-sections in each scanning position image are identified using OCTA images and processed into encoded sub-pixels. Subsequently, cross-sectional images of capillaries are extracted from the repeated scans at each position

Table 1. Summary of Different OCTA and Alternating Scan Imaging Protocols.

	One B-scan time	Repeat times	B-scan number per second
High-speed OCTA	1 ms	4	0.49 vps
OCTA B-scan	1 ms	3	166.7 fps
En-OCTA B-scan	1 ms	1	500 fps

and arranged in chronological order. This procedure generates an encoded image that displays the brightness variations of the capillary cross-sections at the scanning locations, as shown in Fig. 2(d). Adjacent light and dark codes from two scan positions of the same capillary side by side, as shown in Fig. 2(e), exhibit similar brightness variations and a noticeable lag time. Although brightness variations may occasionally be inconsistent, the overall correlation and lag time are clearly observable. The capillary blood velocity V(mm/s) can be calculated after determining the cross-correlation between light and dark encoded images at two locations and establishing the lag time ΔT (s) based on the position where the cross-correlation peak occurred, using a formula:

$$V = \frac{S}{\Delta T + T_B}, \tag{1}$$

where S represents the capillary length between the two scanning positions, which is calculated based on the B-scan interval and the scan voltage between these two positions using the arc calculation method in three-dimensional space[33,34]. T_B is the time difference between two B-scans, 2 ms in our case. Importantly, the sign of ΔT can be either positive or negative, indicating the flow direction. A positive ΔT signifies the directionality of RBC movement from S1 to S2, while a negative ΔT indicates the directionality of RBC movement from S2 to S1.

3. Results and Discussion

Throughout the process of continuous acquisition, capillaries at certain locations on the collected retinal images are observed to partially or completely disappear (see the Visualization 1), showing a pattern of intermittent capillary perfusion similar to that observed by Rosen *et al.*, as shown in Fig. 3(a). At $T = 3.00$ s, a capillary partially disappears [Fig. 3(c)], but it is clearly visible at $T = 2.25$ s [Fig. 3(b)] and $T = 3.75$ s [Fig. 3(d)]. At $T = 23.25$ s, the capillary completely disappears [Fig. 3(f)], yet it is visible at $T = 22.50$ s [Fig. 3(e)] and $T = 24.00$ s [Fig. 3(g)]. These changes may be caused by blood stasis or the absence of RBCs, and although this is a normal physiological phenomenon[35], prolonged occurrences may be associated with neurological disorders such as Parkinson's disease[36].

En-OCTA imaging of the mouse retina was conducted immediately after deep anesthesia was induced in normal mice using sodium pentobarbital. The interval between the two

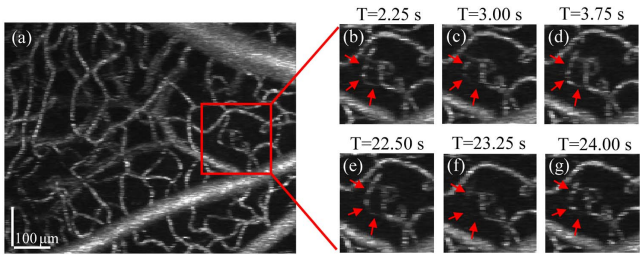

Fig. 3. (a) High-speed OCTA image. (b)–(g) Local magnified images of the same position at different time points.

scanning positions were varied at 12.30, 24.59, 36.89, 49.19, and 61.48 μm, in accordance with the En-OCTA scanning mode and processing methods previously described. Additionally, while maintaining the interval at 61.48 μm, the scanning position spanned the branching points of the capillaries, as illustrated by the red solid lines and green dashed lines in Fig. 2(b). Figure 4 illustrates the brightness encoding of capillaries at different scanning intervals, where an increased delay in capillary blood flow encoding is clearly observed with the widening of scanning intervals.

In Figs. 5(a)–5(f), the peak positions indicating lag time in the correlation analysis consistently correspond with the increase in scanning interval. At the same scanning interval, Fig. 5(e) shows that a distinct peak in the correlation analysis is observed when the scan position does not cross the branch. In contrast, Fig. 5(f) demonstrates that with the scan position crossing the branch, the correlation of capillary brightness encoding rapidly decays, and no distinct peak is evident. Notably, in Figs. 5(a)–5(e), it is observed that as the scanning interval increases, the peak magnitude of the correlation analysis gradually decreases. With the increase in the scanning interval, slight changes in the combination or spacing between individual or groups of RBCs may occur during flow, leading to a decrease in the peaks of the correlation analysis. Despite these changes, the delay in lag time remains clearly visible.

To further validate the proposed method, intraperitoneal anesthesia was administered to mice, followed by the immediate commencement of continuous monitoring of retinal capillary blood flow velocity. Changes in retinal capillary blood flow velocity were measured over time, with measurements repeated

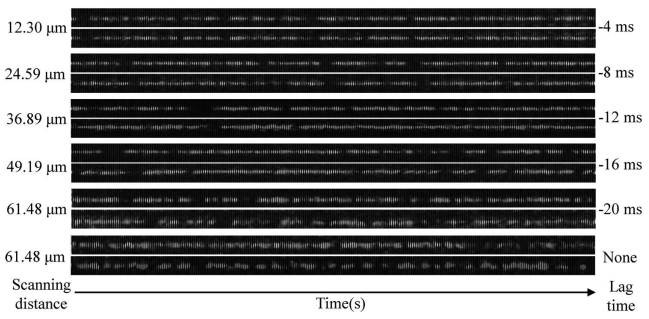

Fig. 4. Encoding of light and dark changes in the same capillary at different scanning intervals.

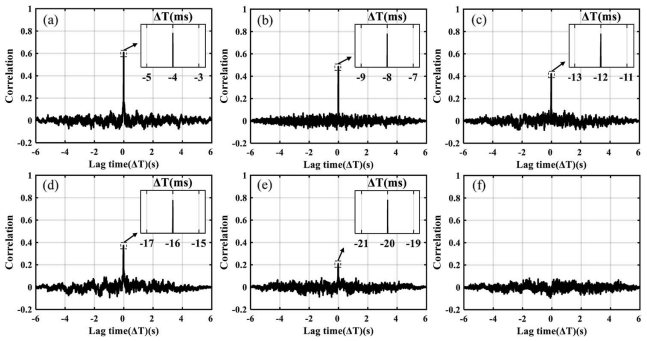

Fig. 5. Correlation of capillary light and dark coding. (a)–(e) Correlation of capillary light and dark coding with equal proportional increase in scanning spacing. (f) Correlation of light and dark coding of scanning positions across bifurcated capillaries.

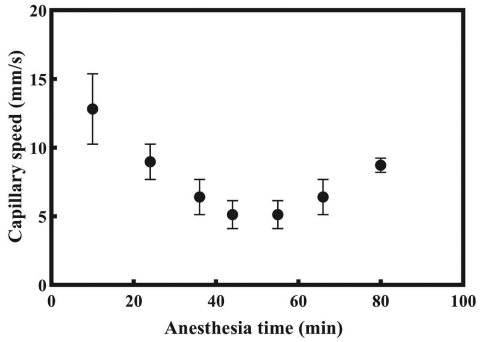

Fig. 6. Changes in blood flow velocity in the same capillaries in the retina of mouse during anesthesia (n = 5, five measurements are taken at each location). Error bars = SEM.

five times at each time point to isolate the brightness encoding of capillary blood flow in the outer plexiform layer (OPL) and to calculate the capillary blood flow velocity.

Figure 6 demonstrates that a significant decline in blood flow velocity within the retinal OPL layer's capillaries occurred as the mice increasingly succumbed to anesthesia. However, as the anesthesia time extended and the effect of the anesthesia gradually decreased, the mice began to regain consciousness, and the blood flow velocity in the capillaries of the OPL layer gradually increased. This is consistent with the capillary blood flow velocity changes in the OPL layer detected by fluorescein angiography using the depth of anesthesia[29] and is also similar to the results measured by Joseph *et al.*[25] using adaptive optics imaging technology.

4. Conclusion

To summarize, this study proposes a non-invasive method for measuring capillary blood flow velocity. This method utilizes high-speed high-resolution OCTA technology and the characteristic of RBCs moving in a single file within capillaries to create a brightness encoding of capillary blood flow. By performing

a correlation analysis on the light and dark encodings at two positions, the lag time is determined based on the peak of the correlation analysis, and by combining this with the length of the capillary between the two scanning points, the absolute velocity of blood flow within the capillaries can be accurately calculated. The field of view of this method is related to the size of the scanning area. As long as the capillaries at two different scanning locations are captured, the blood flow velocity can be calculated using the described method. The newly introduced method is expected to become a valuable tool for studying retinal capillary blood flow velocity. However, scanning two locations using this method introduces selectivity in capillary orientation. If the capillary direction is parallel to the scanning direction, obtaining a clear encoded image may prove challenging. This limitation can be addressed by modifying the scanning protocol to include both horizontal and vertical scans. Future developments could involve adjustments to the scanning scheme and precise measurements of capillary length, enabling non-invasive assessments of regional retinal capillary blood flow velocity. Such advancements would facilitate the detection of average capillary blood flow velocity within specific areas, opening new avenues for studying retinal hemodynamics and the early diagnosis of retinal diseases.

Disclosures

The authors declare no conflicts of interest.

Data availability

Data underlying the results presented in this paper are not publicly available at this time but may be obtained from the authors upon reasonable request.

Acknowledgements

This work was supported by the National Natural Science Foundation of China (Nos. 62205181 and 51975336), the Natural Science Foundation of Shandong Province (No. ZR2022QF017), the Shandong Province Outstanding Youth Science Fund Project (Overseas) (No. 2023HWYQ-023), and the Taishan Scholar Foundation of Shandong Province (No. tsqn202211038).

References

1. W. Liu, S. Wang, B. Soetikno, *et al.*, "Increased retinal oxygen metabolism precedes microvascular alterations in type 1 diabetic mice," Investig. Opthalmology Vis. Sci. **58**, 981 (2017).
2. S. Selvam, T. Kumar, and M. Fruttiger, "Retinal vasculature development in health and disease," Prog. Retin. Eye Res. **63**, 1 (2018).
3. E. Courtie, T. Veenith, A. Logan, *et al.*, "Retinal blood flow in critical illness and systemic disease: a review," Ann. Intensive Care **10**, 152 (2020).
4. A. J. Rong, S. S. Swaminathan, E. A. Vanner, *et al.*, "Predictors of neovascular glaucoma in central retinal vein occlusion," Am. J. Ophthalmol. **204**, 62 (2019).
5. J. Tam, K. P. Dhamdhere, P. Tiruveedhula, *et al.*, "Disruption of the retinal parafoveal capillary network in type 2 diabetes before the onset of diabetic retinopathy," Invest. Ophthalmol. Vis. Sci. **52**, 9257 (2011).
6. J. Tam, K. P. Dhamdhere, P. Tiruveedhula, *et al.*, "Subclinical capillary changes in non-proliferative diabetic retinopathy," Optom. Vis. Sci. **89**, E692 (2012).
7. S. A. Burns, A. E. Elsner, T. Y. Chui, *et al.*, "In vivo adaptive optics microvascular imaging in diabetic patients without clinically severe diabetic retinopathy," Biomed. Opt. Express **5**, 961 (2014).
8. B. Gu, X. Wang, M. D. Twa, *et al.*, "Noninvasive in vivo characterization of erythrocyte motion in human retinal capillaries using high-speed adaptive optics near-confocal imaging," Biomed. Opt. Express **9**, 3653 (2018).
9. J. Tam, J. A. Martin, and A. Roorda, "Noninvasive visualization and analysis of parafoveal capillaries in humans," Invest. Ophthalmol. Vis. Sci. **51**, 1691 (2010).
10. D. Huang, E. A. Swanson, C. P. Lin, *et al.*, "Optical coherence tomography," Science **254**, 1178 (1991).
11. W. Song, L. Zhou, S. Zhang, *et al.*, "Fiber-based visible and near infrared optical coherence tomography (vnOCT) enables quantitative elastic light scattering spectroscopy in human retina," Biomed. Opt. Express **9**, 3464 (2018).
12. J. Wang, S. Nolen, W. Song, *et al.*, "A dual-channel visible light optical coherence tomography system enables wide-field, full-range, and shot-noise limited human retinal imaging," Commun. Eng. **3**, 1 (2024).
13. Y. Jia, O. Tan, J. Tokayer, *et al.*, "Split-spectrum amplitude-decorrelation angiography with optical coherence tomography," Opt. Express **20**, 4710 (2012).
14. T. T. Hormel and Y. Jia, "OCT angiography and its retinal biomarkers," Biomed. Opt. Express **14**, 4542 (2023).
15. Y. Li, W. J. Choi, W. Wei, *et al.*, "Aging-associated changes in cerebral vasculature and blood flow as determined by quantitative optical coherence tomography angiography," Neurobiol. Aging **70**, 148 (2018).
16. A. Wylegala, S. Teper, D. Dobrowolski, *et al.*, "Optical coherence angiography: a review," Medicine **95**, e4907 (2016).
17. Y. Zhao, Z. Chen, C. Saxer, *et al.*, "Phase-resolved optical coherence tomography and optical Doppler tomography for imaging blood flow in human skin with fast scanning speed and high velocity sensitivity," Opt. Lett. **25**, 114 (2000).
18. M. Wan, S. Liang, X. Li, *et al.*, "Dual-beam delay-encoded all fiber doppler optical coherence tomography for in vivo measurement of retinal blood flow," Chin. Opt. Lett. **20**, 011701 (2022).
19. S. Desissaire, F. Schwarzhans, M. Salas, *et al.*, "Analysis of longitudinal sections of retinal vessels using doppler OCT," Biomed. Opt. Express **11**, 1772 (2020).
20. J. Tang, S. E. Erdener, B. Fu, *et al.*, "Capillary red blood cell velocimetry by phase-resolved optical coherence tomography," Opt. Lett. **42**, 3976 (2017).
21. X. Guo, G. Ren, and J. Tang, "Autocorrelation analysis-based OCT velocimetry for axial blood flow velocity imaging of the cerebral capillary network," Opt. Lett. **48**, 3599 (2023).
22. V. J. Srinivasan, H. Radhakrishnan, E. H. Lo, *et al.*, "OCT methods for capillary velocimetry," Biomed. Opt. Express **3**, 612 (2012).
23. W. J. Choi, Y. Li, W. Qin, *et al.*, "Cerebral capillary velocimetry based on temporal OCT speckle contrast," Biomed. Opt. Express **7**, 4859 (2016).
24. Y. Hwang, J. Won, A. Yaghy, *et al.*, "Retinal blood flow speed quantification at the capillary level using temporal autocorrelation fitting OCTA," Biomed. Opt. Express **14**, 2658 (2023).
25. A. Joseph, A. Guevara-Torres, and J. Schallek, "Imaging single-cell blood flow in the smallest to largest vessels in the living retina," eLife **8**, e45077 (2019).
26. A. Joseph, C. J. Chu, G. Feng, *et al.*, "Label-free imaging of immune cell dynamics in the living retina using adaptive optics," eLife **9**, e60547 (2020).
27. R. Liu, X. Wang, S. Hoshi, *et al.*, "High-speed measurement of retinal arterial blood flow in the living human eye with adaptive optics ophthalmoscopy," Opt. Lett. **48**, 1994 (2023).
28. S. Neriyanuri, P. Bedggood, R. C. A. Symons, *et al.*, "Validation of an automated method for studying retinal capillary blood flow," Biomed. Opt. Express **15**, 802 (2024).
29. W. Song, L. Zhou, and J. Yi, "Volumetric fluorescein angiography (vFA) by oblique scanning laser ophthalmoscopy in mouse retina at 200 B-scans per second," Biomed. Opt. Express **10**, 4907 (2019).

30. D. G. Lyons, A. Parpaleix, M. Roche, *et al.*, "Mapping oxygen concentration in the awake mouse brain," eLife **5**, e12024 (2016).
31. W. Yi, K. Hu, Y. Wan, *et al.*, "A high-speed near-infrared optical coherence tomography angiography system for mouse retina," J. Lumin. **270**, 120550 (2024).
32. R. K. Wang, S. L. Jacques, Z. Ma, *et al.*, "Three dimensional optical angiography," Opt. Express **15**, 4083 (2007).
33. A. Poggio and M. Edmund, Integral Equation Solutions of Three-Dimensional Scattering Problems (Computer Techniques for Electromagnetics, 1973).
34. W. Lotmar, A. Freiburghaus, and D. Bracher, "Measurement of vessel tortuosity on fundus photographs," Albrecht Von Graefes Arch. Für Klin. Exp. Ophthalmol. **211**, 49 (1979).
35. J. Li, D. Wang, J. Pottenburgh, A. J. Bower, *et al.*, "Visualization of erythrocyte stasis in the living human eye in health and disease," iScience **26**, 105755 (2023).
36. N. Korte, R. Nortley, and D. Attwell, "Cerebral blood flow decrease as an early pathological mechanism in Alzheimer's disease," Acta Neuropathol. **140**, 793 (2020).